

Direct calculation of correlated absorption amplitudes for Nd:LiYF₄Daniel Åberg,^{1,2} Sverker Edvardsson,¹ and Magnus Engholm¹¹*Department of Physical Electronics/Photonics, ITM, Mid Sweden University, S-851 70 Sundsvall, Sweden*²*Condensed Matter Theory Group, Uppsala University, Box 530, S-751 21 Uppsala, Sweden*

(Received 22 January 2003; published 6 November 2003)

The correlation contribution to the transition amplitudes are investigated in the case of Nd:LiYF₄. By using many-body perturbation theory, we derive expressions for an effective dipole operator. The operators considered are $\Omega_{es}^{(1)\dagger} D \Omega_{cf}^{(1)}$, $\Omega_{cf}^{(1)\dagger} D \Omega_{es}^{(1)}$, $\Omega_{es-cf}^{(2)\dagger} D$, and $D \Omega_{es-cf}^{(2)}$. In contrast to third-order spin-orbit and crystal-field modified amplitudes, inclusion of correlation modifies the standard second-order amplitudes significantly. A model cluster is optimized to experimental energy levels. This approach is then used to compute consistent odd and even crystal-field parameters needed for theoretical absorption spectra. As expected, it is observed that transitions occurring at small wavelengths are quite heavily influenced by correlation. The overall agreement between experimental and theoretical spectra below 600 nm (above 17000 cm⁻¹) is greatly improved when correlation is taken into account.

DOI: 10.1103/PhysRevB.68.195105

PACS number(s): 78.20.Bh, 32.70.Cs, 78.40.-q

I. INTRODUCTION

Rare-earth (RE) metals play a fundamentally important role in modern optical technology. A few examples are REs in laser materials, optical fiber amplifiers, and semiconductors. What they all have in common is that the REs are in one way or another subject to a crystal field (cf) from their chemical environment leading to various optical properties. Certain transitions can change dramatically from one host material to another. In, for example, a RE-doped fiber amplifier, there are always losses such as destructive up-conversion or energy transfer (e.g., high Er concentrations), accidental degeneracy that can lead to excited state absorption, bad radiative or nonradiative transitions, amplified spontaneous emission, etc. The material or the chemical environments can certainly be altered, but in what direction? A good physical understanding requires, first, a knowledge of the electronic structure of the RE ion itself and, second a knowledge of the chemical structure. It is important to test and develop reliable theoretical methods. A good foundation is, for example, crucial to enable us to optimize RE clusters to give certain desired optical properties.

In a previous paper¹ we investigated second and third order contributions (cf-cf and cf-spin-orbit perturbations) to the *f-f* transition amplitudes in the case of a few rare-earth ions in YLF (LiYF₄). Quite a good agreement between theory and experiment was achieved. It was shown that these third-order contributions are in practise small for YLF. The question was then raised whether third-order correlation effects will also be unimportant. The present work will attempt to address this rather intricate question.

It is nontrivial to use *the perturbed functions approach* applied in the previous work, because of the two-particle nature of the electron correlation. Here, we shall instead employ the traditional many-body perturbation theory (MBPT). Smentek-Mielczarek and Hess² earlier studied third-order intensity parametrization in the case of Pr in a variety of hosts: LaAlO₃, NdAlO₃ and LaCl₃. General discussions about correlation effects for several RE ions are available in Ref. 3; also see references therein. Also, the correlation contribu-

tions using the velocity form of the dipole operator in the case of Eu in *C*_{2v} and *C*_{3v} symmetry were studied in Refs. 4 and 5. In Ref. 6, Smentek presents a survey of published approaches for one- and two-photon transitions. Various discussions by Reid and co-workers may also be found in Refs. 7 and 8. The general trend is that correlation probably is quite important for the evaluation of *f-f* transition intensities. This conclusion will also be emphasized in the present work.

II. MBPT APPROACH FOR AN EFFECTIVE DIPOLE OPERATOR

The basic dipole oscillator strength for a transition $\psi_i \rightarrow \psi_f$ is proportional to

$$P_q \propto \nu_{if} |\langle \psi_i | D_q^1 | \psi_f \rangle|^2; \quad (1)$$

see, e.g., Ref. 9. It is in general assumed that good, physical Stark wave functions and energies for rare-earth (or actinide) crystal ions can be obtained by diagonalizing the Hamiltonian

$$H = \sum_i \left(-\frac{1}{2} \nabla_i^2 - \frac{Z}{r_i} \right) + \sum_{i < j} \frac{1}{r_{ij}} + \sum_i \xi(r_i) l_i \cdot s_i \\ + \sum_i \sum_{tp} A_{tp} r_i^t C_{tp}(\theta_i, \phi_i) \quad (2)$$

in atomic units. The last term is a single-particle ansatz to take into account the influence of the crystal field. The exact eigenfunctions of *H* are here denoted ψ_a . However, the size of the calculation forces us to employ a limited basis set of *f*-type angular functions for *N* equivalent *f* electrons. This reduction is usually accomplished by introducing an effective Hamiltonian *H*_{eff}; diagonalization then results in exact eigenvalues and the model functions ψ_a^0 that are projections of the exact ψ_a ; see Ref. 10. However, in a pure *f* space, all matrix elements $\langle \psi_i^0 | D_q^1 | \psi_f^0 \rangle$ are identically zero due to parity. In order to estimate the transition intensities within this space, we can construct an effective dipole operator *D*_{eff}. In

the following we will make use of the wave operator,¹⁰ defined by $\psi_a = \Omega \psi_a^0$. We shall now show a simple, yet illustrative, example of an effective operator (D is short for D_q^1):

$$\langle \psi_i | D | \psi_f \rangle = \langle \Omega \psi_i^0 | D | \Omega \psi_f^0 \rangle = \langle \psi_i^0 | \Omega^\dagger D \Omega | \psi_f^0 \rangle.$$

Encouraged by this, one could identify $\Omega^\dagger D \Omega$ as a candidate for D_{eff} . Unfortunately, this operator contains unlinked diagrams and also suffers from problems with orthogonality. Instead we will follow a more suitable approach, for example that proposed by Duan and Reid:¹¹

$$D_{eff} = (\Omega^\dagger \Omega)^{-1} \Omega^\dagger D \Omega. \quad (3)$$

This operator is linked and does not have orthogonality problems. By using the standard expansion $\Omega = \sum_{i=0}^{\infty} \Omega^{(i)}$,¹⁰ we write the non-vanishing terms of Eq. (3) up to third order ($D_{eff}^{(1)}$ does not contribute to the amplitudes):

$$D_{eff}^{(2)} = D \Omega_{cf}^{(1)} + \Omega_{cf}^{(1)\dagger} D \quad (4)$$

$$D_{eff}^{(3)} = \Omega_{es}^{(1)\dagger} D \Omega_{cf}^{(1)} + \Omega_{cf}^{(1)\dagger} D \Omega_{es}^{(1)} + \Omega_{cf-es}^{(2)\dagger} D + D \Omega_{cf-es}^{(2)}. \quad (5)$$

The subindices cf and es denote crystal field and electrostatic interactions. The wave operators $\Omega^{(i)}$ can be obtained using the linked-diagram theorem for open shell systems.¹⁰ To obtain explicit expressions for $D_{eff}^{(2)}$ and $D_{eff}^{(3)}$, we use the second quantized form of the operators and apply Wick's theorem^{12,13} for products of creation and annihilation opera-

tors of normal form. This leads to a great number of zero-, one- and two-particle operators. They are available by request from the authors. The zero-particle operators do not contribute to the transition amplitude. The second-order operator $D_{eff}^{(2)}$ was discussed in a previous paper.¹ To second order, MBPT and the *perturbed functions approach* effectively yield the same result. For third-order contributions we shall focus on mixing of intraelectron correlations with the crystal field. Other third-order effects such as spin-orbit or higher crystal-field interactions have previously been studied in Refs. 1 and 14, and references therein.

The electrostatic interactions result in 82 nonvanishing one-particle operators for $D_{eff}^{(3)}$. These, along with the contributions from $D_{eff}^{(2)}$, can be written in the one-particle parametrization scheme of Reid and Richardson,¹⁵

$$D_1 = \sum_{\lambda t p} A_{tp}^\lambda U_{t+p}^{(\lambda)} (-1)^q \langle \lambda(p+q), 1-q | t p \rangle, \quad (6)$$

where $\lambda = 2, 4, 6$ and $t = \lambda \pm 1$. This is accomplished by applying the theorems of Jucys *et al.*¹⁶ or El Baz and Castel¹⁷ for separable diagrams.

Because of space restrictions, here we shall list only one contribution to A_{tp}^λ . We let a denote a core orbital, r and s denote excited or valence orbitals, and m and n denote valence orbitals only. Note that ϵ_i is a single-particle energy. Two of the diagrams representing parts of the $\Omega_{cf}^{(1)\dagger} D \Omega_{es}^{(1)}$ operator can be expressed as

$$-\sum_{mn} a_m^\dagger a_n \sum_{ars}^{r \neq 4f} \frac{\langle ma | r_{12}^{-1} | rs \rangle \langle s | h_{cf} | n \rangle \langle r | d | a \rangle + \langle sr | r_{12}^{-1} | na \rangle \langle m | h_{cf} | r \rangle \langle a | d | s \rangle}{(\epsilon_{4f} + \epsilon_a - \epsilon_r - \epsilon_s)(\epsilon_{4f} - \epsilon_r)}.$$

The contribution ΔA_{tp}^λ to A_{tp}^λ for even λ can then be obtained after simplification and a recoupling of the angular terms:

$$\begin{aligned} \Delta A_{tp}^\lambda &= 2(2\lambda + 1)(2t + 1)^{-1/2} A_{tp} \sum_{kl a' r' l_s}^{r \neq 4f} (-1)^k \begin{Bmatrix} l & l_r & 1 \\ l_a & l_s & k \end{Bmatrix} \\ &\times \begin{Bmatrix} t & 1 & \lambda \\ l & l & l_r \end{Bmatrix} \langle l_s | \hat{C}^k | l \rangle \langle l_r | \hat{C}^k | l_a \rangle \langle l | \hat{C}^t | l_r \rangle \\ &\times \langle l_a | \hat{C}^1 | l_s \rangle \sum_{n_a n_r n_s}^{n_r l_r \neq 4f} \frac{R^k(sr, 4fa) H^t(4f, r) H^1(a, s)}{(\epsilon_{4f} + \epsilon_a - \epsilon_r - \epsilon_s)(\epsilon_{4f} - \epsilon_r)}. \end{aligned} \quad (7)$$

Here R^k denotes the standard electrostatic Slater integral and H^t is defined by

$$H^t(i, j) = \int P_{n_i l_i} P_{n_j l_j} r^t dr.$$

$\langle l_a | \hat{C}^k | l_b \rangle$ is a reduced matrix element of a renormalized spherical harmonic $C_{kq} = \sqrt{4\pi/(2k+1)} Y_{kq}$. The summation over the radial integrals in Eq. (7) will be further described in Sec. III.

$D_{eff}^{(3)}$ also contains two-particle operators, which are absent in the Judd-Ofelt formulation.^{9,18} This operator contains 31 nonvanishing two-particle operators; these can be expressed in a parametrization scheme similar to the one-particle case by recoupling the angular momenta t and 1 of the crystal field and dipole operator, respectively, to form a tensor operator product of rank λ :

$$\begin{aligned} D_2 &= \sum_{k_1 k_2 \lambda t p} A_{tp}^{(k_1 k_2) \lambda} (-1)^q \langle \lambda(p+q), 1-q | t p \rangle \\ &\times \{ u^{k_1}(1) u^{k_2}(2) \}_{p+q}^\lambda. \end{aligned}$$

Here $0 \leq k_1, k_2 \leq 6$, $0 \leq \lambda \leq 12$, and $1 \leq t \leq 13$. Note that a different parametrization is used in, e.g., Ref. 5:

$$D_2 = \sum_{k_1 k_2 \lambda t p} T_{k_1 k_2 \lambda} \{u^{k_1}(1)u^{k_2}(2)\}_{p+q}^\lambda.$$

However, from an *ab initio* point of view, the choice is a matter of taste. The oscillator strengths can finally be calculated from

$$P_q \propto \nu_{if} |\langle \psi_i^0 | D_1 + D_2 | \psi_f^0 \rangle|^2. \quad (8)$$

III. RADIAL CONTRIBUTION

All contributions to A_{tp}^λ or $A_{tp}^{(k_1 k_2)^\lambda}$ are associated with radial terms which require intensive computational efforts. The magnitudes of all these radial contributions are crucial in order to understand how important the influence of electron correlation actually is for transition intensities. We shall now show how the radial contribution in the example above [Eq. (7)], here denoted by R , is calculated:

$$R = \sum_{n_a n_r n_s}^{n_r l_r \neq 4f} \frac{R^k(sr, 4fa) H^t(4f, r) H^1(a, s)}{(\epsilon_{4f} + \epsilon_a - \epsilon_r - \epsilon_s)(\epsilon_{4f} - \epsilon_r)}.$$

By defining the one- and two-particle perturbed functions

$$\begin{aligned} \rho^t(4f \rightarrow l_r; r_2) &= \sum_{n_r'}^{n_r' l_r \neq 4f} P_{n_r'}(r_2) \frac{H^t(4f, r')}{\epsilon_{4f} - \epsilon_{r'}}, \\ \rho^k(4f, n_a l_a \rightarrow l_s l_r; r_1 r_2) &= \sum_{n_r n_s} P_{n_s}(r_1) P_{n_r}(r_2) \frac{R^k(sr, 4fa)}{\epsilon_{4f} + \epsilon_a - \epsilon_r - \epsilon_s}, \end{aligned}$$

we can write R as a summation over integrals for the perturbed functions:

$$R = \sum_{n_a} \int \int \rho^k(r_1 r_2) \rho^t(r_2) P_{n_a}(r_1) r_1 dr_1 dr_2. \quad (9)$$

It can be seen by inspection that all contributions to A_{tp}^λ and $A_{tp}^{(k_1 k_2)^\lambda}$ have radial parts which can be calculated using perturbed functions. These can be obtained, as initially demonstrated by Sternheimer *et al.*¹⁹ by solving one- or two-particle inhomogeneous Schrödinger equations.^{10,20,21} Here we shall instead employ the method of Salomonson and Öster²² which is better for numerical evaluation (more memory efficient). They utilized the fact that the eigenfunctions of a discretized Hamiltonian

$$\left[-\frac{1}{2} \frac{d^2}{dr^2} + \frac{l(l+1)}{2r^2} - \frac{Z}{r} + u(r) \right] P_{nl} = \epsilon_{nl} P_{nl} \quad (10)$$

are complete. On a grid with M internal points we obtain M eigenvectors. These span the entire functional space on that grid, which means that any discretized function on the same grid can be written exactly as an unique linear combination of the P_{nl} functions. Therefore, by generating *all* solutions to Eq. (10) for a grid with M points, we can directly perform the summations in the expressions for ρ^t and ρ^k and integrate according to Eq. (9) to obtain an estimate $R(M)$ to R . The

limit $R = R(M \rightarrow \infty)$ is approximated by calculating $R(M)$ for a few grids and then applying repeated extrapolations. In order to be able to use grids with as few points as possible, a logarithmic discretization $r = e^x$ of Eq. (10) is used.²² Here $2.3 \times 10^{-6} \leq r \leq 150$ a.u. and the logarithmic step lengths Δx used in the extrapolation scheme were 0.2, 0.1, 0.05, 0.025, and 0.0125. Further, the second derivative was approximated by the central three-point formula and the potential $-Z/r + u(r)$ was chosen as the converged relativistic Hartree-Fock $4f$ potential from Cowan's program *RCN*.²³ The resulting tridiagonal matrices were diagonalized using the LAPACK routine *DSTEVR*.²⁴ This procedure was then applied for the radial contributions to all 103 operators.

IV. CRYSTAL FIELD OPTIMIZATION

In order to compute intensities, access to consistent odd crystal field parameters (CFPs) is a necessity. Standard energy level fittings usually result in good even parameters. The odd parameters, however, are in general difficult to determine. In order to test the correlated expressions above, and to see the influence on theoretical spectra, we shall use an unorthodox approach where a consistent set of parameters is determined for an optimized environment corresponding to the crystal field, but also to some extent to correlation and to charge transfer. Explicitly, the optimization of a model cluster is carried out with respect to the energy levels. We shall then use the optimized parameters to compute consistent odd CFP needed for the correlated oscillator strengths. We set up the model cluster by considering the nearest ligands out to a certain cut off distance (R_{cut}) with the rare-earth ion in the center. This environment is represented by a charge density $n(\vec{R})$ which perturbs the f levels. The parameters A_{tp} are then calculated according to

$$A_{tp} = (-1)^{p+1} \int \frac{n(\vec{R})}{R^{t+1}} C_{t-p}(\theta, \varphi) d\vec{R},$$

where R , θ , and φ are spherical coordinates of a surrounding charge density element. The coordinate system used is described in Ref. 1. To simplify, we shall here only consider the expansion

$$\begin{aligned} A_{tp} \approx & (-1)^{p+1} \sum_j [q_j R_j^{-t-1} \\ & + \mu_j R_j^{-t-2}(t+1)] C_{t-p}(\theta_j, \varphi_j), \end{aligned} \quad (11)$$

where the dipole moment $\mu_j = \alpha_j E_j$ is computed self-consistently as in Ref. 1. We have here disregarded higher moments and the sum is carried out for the surrounding ligands at distances R_j out to R_{cut} . Optimization is done by varying the charges q_j (charge transfer) and the dipole polarizabilities α_j within physical ranges. The relation between standard even crystal field parameters B_{tp} and A_{tp} is expressed as $B_{tp} = \rho_t A_{tp}$ ($t = 2, 4$, and 6), where ρ_t accounts for an effective expansion of the radial f function and shielding. The ρ_t parameters are optimized within certain allowed ranges. The effective Hamiltonian (see Ref. 1)

TABLE I. Optimized parameters for Nd:YLF. F^k , ξ , α , β , γ , T^i , and σ are in units of cm^{-1} . The optimized dipole polarizabilities and the parameters ρ^k are expressed in \AA^3 and atomic units, respectively. For comparison we also list crystal ion polarizabilities (within brackets) by Schmidt *et al.* (Ref. 30) using the Watson sphere model. The B_{ip} parameters (in cm^{-1}) are obtained from $B_{ip} = \rho_i A_{ip}^{opt}$; see Table II.

Parameter	Parameter	Parameter	Parameter	Parameter	Parameter
F^2	72930.3	T^2	274.9	α_{Li^+}	0.041 (0.0321)
F^4	52379.5	T^3	96.3	$\alpha_{\text{Y}^{3+}}$	1.14 (0.87)
F^6	35169.6	T^4	142.3	α_{F^-}	0.47 (0.731)
ξ	874.2	T^6	-295.3	ρ_2	0.81
α	20.7	T^7	352.4	ρ_4	4.23
β	-559.7	T^8	174.6	ρ_6	54.8
γ	1520.0	N	149	σ	26.1
B_{20}	367.0	B_{40}	-762.3	B_{44}	1313.4
B_{60}	-0.2	$\text{Re } B_{64}$	1030.9	$\text{Im } B_{64}$	160.8

$$H_{eff} = \sum_{k=2,4,6} f_k F^k + \sum_i \xi(r_i) l_i \cdot s_i + \alpha L^2 + \beta G(G_2) + \gamma G(R_7) + \sum_{i=2,3,4,6,7,8} t_i T^i + \sum_i \sum_{ip} B_{ip} C_{ip}(\theta_i, \phi_i)$$

is then repeatedly diagonalized using the software *lanthanide*,²⁵ until optimized Stark energies are obtained (experimental energies from Ref. 26). All parameters are varied simultaneously. Besides variations of the usual free ion spin-orbit and correlation parameters ($\xi, F^2, F^4, F^6, \alpha, \beta, \gamma, T^2, T^3, T^4, T^6, T^7, T^8$), we also vary (q_j, α_j, ρ_j). This optimization problem is nonlinear so it is slightly more involved to obtain solutions compared to standard matrix formulations. Here we have chosen to apply a global optimization method, adaptive simulated annealing; see Ref. 27. We are applying this model to Nd:LiYF₄; see Ref. 1 for more details. We form the model cluster of radius $R_{cut} = 30$ with ligand positions obtained from Ref. 28 and with the RE ion at the origin. For neutrality we also require $q_{\text{Li}} + q_{\text{Y}} + 4q_{\text{F}} = 0$, thus reducing the number of free parameters to 21. Although it would be desirable to use a larger value for R_{cut} , this choice is beneficial for computational speed and is mainly approximate for lower order parameters only, i.e., A_{20} in YLF ($A_{1p} \equiv 0$ in S_4 symmetry). After a series of convergence tests, we found that this approximation is good within a few percent. Initially we allowed the effective charges to vary but found that optimal values were actually obtained very near the formal charges. The optimization was then continued by using formal charges thus reducing the number of parameters to 19. In Table I we tabulate the resulting optimized parameter values. The quality of a fit is often measured in terms of σ , defined by

$$\sigma = \sqrt{\sum_i^N \frac{(E_{i,fit} - E_{i,exp})^2}{N - P}}$$

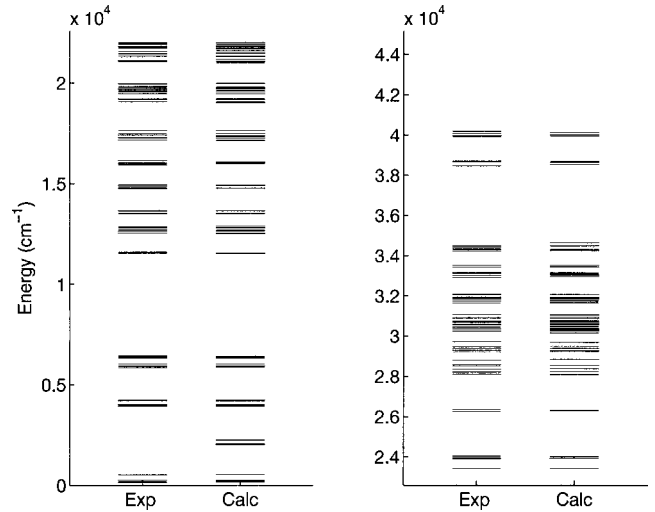


FIG. 1. Experimental and optimized theoretical energy levels in cm^{-1} for Nd:YLF.

where N is the number of energy levels and P is the number of free parameters used. Here we obtained quite a good fit, $\sigma = 26.1 \text{ cm}^{-1}$ (19 parameters), which can be compared with the value $\sigma = 27.6 \text{ cm}^{-1}$ in Ref. 26 where instead a direct variation of B_{ip} was carried out (a total of 27 parameters were employed in that work). We have thus optimized a model cluster that gives good agreement with the experimental energy levels; see Fig. 1. Equation (11) can now be used for generating either even or odd crystal field parameters; see Table II. In Sec. V we shall use these odd parameters, consistent with the optimized even parameters, to compute correlated transition intensities.

V. SIMULATION OF ABSORPTION SPECTRA

By using the radial integrals and the optimized crystal field, we can now calculate the contributions to the intensity

TABLE II. A_{ip} parameters given in atomic units for Nd:YLF. The first parameter set A_{ip}^{old} is taken from Table III of Ref. 1 (Note that all the odd parameters have changed sign due to typographical errors in Ref. 1). The second set is optimized using the procedure described in the present work. All parameters are rotated in the R approach (Ref. 31) according to $e^{-ip\alpha} A_{ip}$ such that $\text{Im } A_{44} = 0$ ($\alpha = 34^\circ$).

tp	$\text{Re } A_{ip}^{old}$	$\text{Im } A_{ip}^{old}$	$\text{Re } A_{ip}^{opt}$	$\text{Im } A_{ip}^{opt}$
10	2.00×10^{-2}	-	-	-
11	4.17×10^{-3}	2.63×10^{-2}	-	-
20	3.44×10^{-3}	-	2.059×10^{-3}	-
32	2.04×10^{-4}	-1.05×10^{-4}	7.52×10^{-4}	3.34×10^{-4}
40	-1.83×10^{-3}	-	-8.22×10^{-4}	-
44	2.90×10^{-3}	-	1.42×10^{-3}	-
52	-1.40×10^{-3}	-3.79×10^{-5}	-5.87×10^{-4}	7.42×10^{-6}
60	4.85×10^{-6}	-	-1.94×10^{-8}	-
64	2.39×10^{-4}	3.08×10^{-5}	8.58×10^{-5}	1.34×10^{-5}
72	3.20×10^{-6}	-1.90×10^{-6}	6.09×10^{-7}	-8.26×10^{-7}
76	6.51×10^{-5}	-8.67×10^{-6}	1.70×10^{-5}	-2.76×10^{-6}

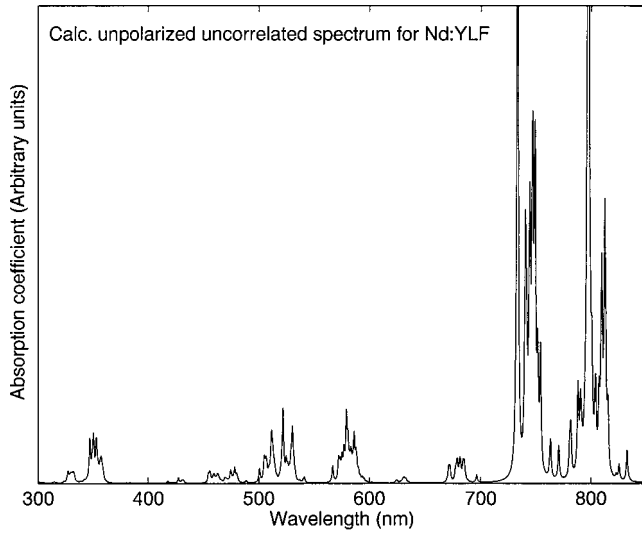


FIG. 2. Theoretical unpolarized uncorrelated absorption spectrum for Nd:YLF.

parameters from the correlated dipole operators. Theoretical values of the A_{tp}^λ and $A_{tp}^{(k_1 k_2)\lambda}$ for Nd:YLF are available on request from the authors (thousands). It should be noted that the dipole operators were generated using the $4f$ relativistic Hartree-Fock potential, and thus the main part of the spherical correlation is already accounted for. It is well known that the Hartree-Fock method is very efficient with regard to accounting for spherical correlation. By taking the Hartree-Fock level as the point of departure, we omit all spherical corrections to the operators arising in MBPT. It is thus beneficial to remove the terms with $k=0$ in the expansion of r_{12}^{-1} as well as the effective potential defined by

$$\langle i|v|j\rangle = \langle i|-u|j\rangle + \sum_a^{occ} (\langle ia|r_{12}^{-1}|ja\rangle - \langle ia|r_{12}^{-1}|aj\rangle).$$

To proceed, the oscillator strengths of Eq. (8) are then calculated for transitions from the ground state to the excited states using the optimized Stark wave functions and energies described in Sec. IV. The ground state is also assumed to be thermally populated at 300 K; see Eq. (2) in Ref. 1. An unpolarized absorption spectrum is generated using

$$L(\lambda)\lambda_0^2 \sum_{q=-1}^1 P_q \propto \int \alpha(\lambda) d\lambda,$$

where $L(\lambda)$ is a Lorentzian function:

$$L(\lambda) = \frac{1}{\pi} \frac{\frac{1}{2}\Gamma}{(\lambda - \lambda_0)^2 + \left(\frac{1}{2}\Gamma\right)^2}.$$

In Figs. 2 and 3, we display the uncorrelated (method in Ref. 1) and the present correlated theoretical absorption spectra, respectively. The full width at half maximum parameter Γ used in the Lorentzian broadening was chosen as 1.5 nm. An experimental plot of an unpolarized absorption spectrum is

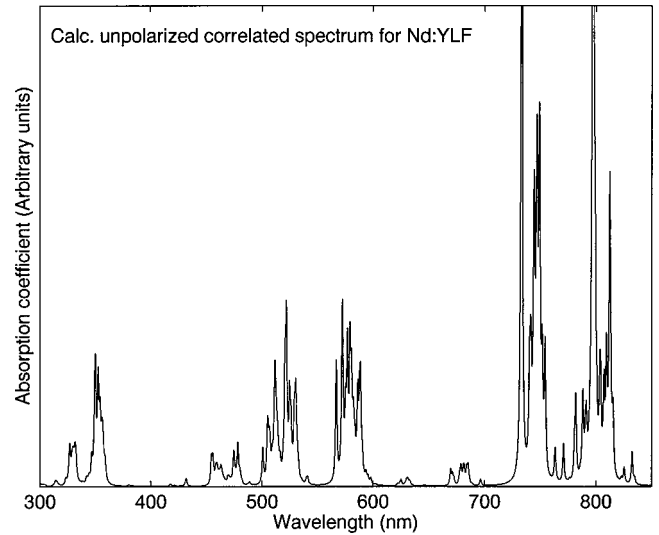


FIG. 3. Theoretical unpolarized correlated absorption spectrum for Nd:YLF.

displayed in Fig. 4. This experimental data are available from NASA LSB's Database Lasers²⁹ $[(2\sigma + \pi)/3]$. We observe that the theoretical spectra are essentially identical above 600 nm, indicating that correlation effects for these bands are insignificant. This region is also in very nice agreement with experiment. At wavelengths below 600 nm, the agreement between the theoretical uncorrelated spectrum (Fig. 2) and the experimental spectrum (Fig. 4) is poor. However, we see that the transitions below 600 nm are greatly improved by correlation interaction (Fig. 3). This is not surprising since these final states are those closest to the excited configurations. The overall agreement between Figs. 3 and 4 is convincing, indicating that the determined A_{tp} parameters in Table II are probably of high standard. The low magnitudes of the uncorrelated oscillator strengths below 600 nm were also noted in the previous work.¹ Most of these transi-

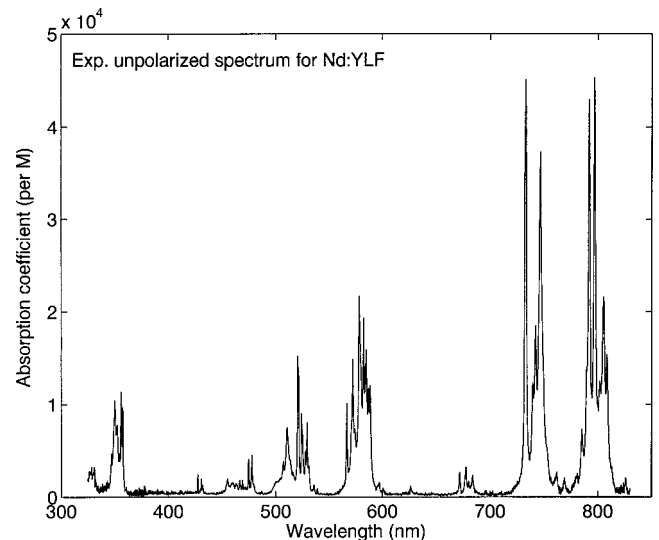


FIG. 4. Experimental unpolarized absorption spectrum for Nd:YLF.

tions mainly depend on A_{1p} and A_{3p} . However, the point symmetry S_4 for the rare-earth ion site in YLF renders $A_{1p} \equiv 0$. In the previous paper it was argued that perhaps the dynamic environment causes the symmetry to break, allowing the use of a nonzero value for A_{1p} . The present work shows that these low oscillator strengths are greatly rectified by taking electron correlation into account. A dynamical explanation can nevertheless not be discarded, although it would seem that its contribution is considerable smaller than previously thought.

VI. CONCLUSION

We have formulated a theory for correlated transition amplitudes. We also suggest an unorthodox but consistent approach for the treatment of the crystal field. Excellent agreement with the experimental spectrum for Nd:YLF is observed. It is expected that this approach will also work for other near ionic laser crystals. If this approach turns out to yield good results in future simulations, it may be especially useful in finding interesting rare-earth clusters with certain

designed optical properties desired in technological applications. For example, work is now in progress to find efficient chemical rare-earth clusters that can be doped into optical fibers for use as efficient fiber amplifiers. It should also be noted that the correlated approach presented here can be further improved. One possibility is to revert to “exact” solutions of the Schrödinger equation, often used for light atoms. This type of approach is presently being investigated by us for Pr, Nd, and Er. The advantage of an “exact” approach compared to MBPT is actually its greater simplicity. Although we feel that such an approach is interesting at a fundamental level, it is probably less so from a technological point of view.

ACKNOWLEDGMENTS

This work was supported by grants from the Swedish Research Council (VR) and the KK foundation (KKS). Support from B. Johansson and O. Eriksson (Uppsala University) is also appreciated. The optimization library software was developed by Lester Ingber and other contributors.

-
- ¹D. Åberg and S. Edvardsson, Phys. Rev. B **65**, 045111 (2002).
²L. Smentek-Mielczarek and B.A. Hess, J. Chem. Phys. **87**, 3509 (1987).
³L. Smentek-Mielczarek and B.A. Hess, J. Chem. Phys. **89**, 703 (1988).
⁴L. Smentek and B.A. Hess, Mol. Phys. **92**, 835 (1997).
⁵L. Smentek and B.A. Hess, Mol. Phys. **92**, 847 (1997).
⁶L. Smentek, Spectrochim. Acta, Part A **54**, 1545 (1998).
⁷M.F. Reid and B. Ng, Mol. Phys. **67**, 407 (1989).
⁸M.F. Reid, J. Alloys Compd. **193**, 160 (1993).
⁹B.R. Judd, Phys. Rev. **127**, 750 (1962).
¹⁰I. Lindgren and J. Morrison, *Atomic Many-Body Theory*, 2nd ed. (Springer, New York, 1985).
¹¹C.K. Duan and M.F. Reid, J. Chem. Phys. **115**, 8279 (2001).
¹²G.C. Wick, Phys. Rev. **80**, 268 (1950).
¹³J. Paldus and J. Čížek, Adv. Quantum Chem. **9**, 105 (1975).
¹⁴L. Smentek and B.A. Hess, Mol. Phys. **88**, 783 (1996).
¹⁵M.F. Reid and F.S. Richardson, J. Phys. Chem. **88**, 3579 (1984).
¹⁶A.P. Jucys (Yutsis), I.B. Levinson, and V.V. Vanagas, *Mathematical Apparatus of the Theory of Angular Momentum* (Israel Program for Scientific Translations, Jerusalem, 1962).
¹⁷E. El Baz and B. Castel, *Graphical Methods of Spin Algebras in Atomic, Nuclear, and Particle Physics* (Dekker, New York, 1972).
¹⁸G.S. Ofelt, J. Chem. Phys. **37**, 511 (1962).
¹⁹R.M. Sternheimer, M. Blume, and R.F. Peierls, Phys. Rev. **173**, 376 (1968).
²⁰A.M. Mårtensson, J. Phys. B **12**, 3995 (1979).
²¹A.M. Mårtensson-Pendrill, in *Numerical Determination of the Electronic Structure of Atoms, Diatomic and Polyatomic Molecules*, edited by M. Defranceschi and J. Delhalle (Kluwer, Dordrecht, 1989), pp. 131–160.
²²S. Salomonson and P. Öster, Phys. Rev. A **40**, 5559 (1989).
²³Program available at <ftp://aphysics.lanl.gov/pub/cowan>
²⁴Program library available at <http://www.netlib.org/lapack>
²⁵S. Edvardsson and D. Åberg, Comput. Phys. Commun. **133**, 396 (2001).
²⁶H. de Leebeek and C. Görller-Walrand, J. Alloys Compd. **275-277**, 407 (1998).
²⁷Program available at <http://www.ingber.com>.
²⁸E. Garcia and R.R. Ryan, Acta Crystallogr., Sect. C: Cryst. Struct. Commun. **49**, 2053 (1993).
²⁹see <http://aesd.larc.nasa.gov/gl/laser/dbmain.htm>
³⁰P.C. Schmidt, A. Weiss, and T.P. Das, Phys. Rev. B **19**, 5525 (1979).
³¹C. Rudowicz and J. Qin, Phys. Rev. B **67**, 174420 (2003).